Pergamon

Tetrahedron: *Asymmetry* 9 (1998) 1899–1916

TETRAHEDRON: *ASYMMETRY*

Biotransformation of organic sulfides. Predictive active site models for sulfoxidation catalysed by 2,5-diketocamphane 1,2-monooxygenase and 3,6-diketocamphane 1,6-monooxygenase, enantiocomplementary enzymes from *Pseudomonas putida* NCIMB 10007

Jean Beecher and Andrew Willetts *

Department of Biological Sciences, University of Exeter, Exeter, Devon EX4 4PS, UK

Received 18 March 1998; accepted 28 April 1998

Abstract

Growth of the bacterium *Pseudomonas putida* NCIMB 10007 on racemic camphor induces two enantiocomplementary diketocamphane monooxygenase isofunctional enzymes (isozymes) both able to catalyse electrophilic biooxidation of a wide range of prochiral sulfoxides to the corresponding chiral sulfoxides. Active site models to explain and predict the stereoselectivity of the sulfoxidations catalysed by both isozymes are proposed. The models are based on restrictive space descriptors derived from the optimised outcomes obtained with 23 different phenyl alkyl, benzyl alkyl, methyl alkyl and ethyl alkyl sulfides: consistency was maximised by using the same enzyme preparations throughout. The models, which are consistent with the recognised stereoselectivities of diketocamphane monooxygenase catalysed nucleophilic biooxidations of ketones to lactones, are the first to provide insight into the active site topography of FMN plus NADH-dependent Baeyer–Villiger monooxygenases. In addition, they are unique in providing a direct comparison of the active sites of two enantiocomplimentary isofunctional proteins that have evolved in the same cell line.

1. Introduction

The Baeyer–Villiger monooxygenases (BVMOs) are an interesting group of flavoprotein enzymes (EC 1.14.13.x) with considerable proven potential for yielding key chiral synthons for chemoenzymatic synthesis.[1] Intriguingly, these enzymes exhibit the rare characteristic of being able to catalyse two mechanistically different types of biochemical reactions within the confines of the same active site. Originally recognised for their ability to promote the nucleophilic oxygenation of ketones and aldehydes

* Corresponding author. E-mail: A.J.Willetts@exeter.ac.uk

0957-4166/98/$19.00
PII: S0957-4166(98)00174-8

in a manner analogous to the peracid-catalysed chemical reaction from which they take their name,[2] more recently it has been recognised that these enzymes can also catalyse the electrophilic oxygenation of heteroatoms such as sulfur.[3]

Based on both N-terminal amino acid sequence data and other biochemical characteristics, these biocatalysts have been categorised as either NADPH plus FAD-dependent Type 1 or NADH plus FMN-dependent Type 2 enzymes.[1,4] Studies conducted with the purified Type 1 enzyme cyclohexanone monooxygenase (CHMO) from cyclohexanol-grown *Acinetobacter calcoaceticus* NCIMB 9871, a monomeric 59kDa protein shown to possess a single active site,[5] have confirmed that both nucleophilic[6] and electrophilic[7] biooxidations can proceed with exquisite selectivity to yield various homochiral products that have served as synthons or chiral auxiliaries in the subsequent elaboration of a wide variety of useful compounds.[8]

It is advantageous to be able to assess the synthetic utility of an enzyme by predicting the regio- and stereochemical outcome of proposed biotransformations. The most relevant progress to date on BVMOs has been reported with the Type 1 enzyme CHMO from *A. calcoaceticus* NCIMB 9871. Although the full amino acid sequence is known and the enzyme has been cloned,[9] no 3D structure of the enzyme, including the dimensions of the active site, has yet been established. However, various models of the active site topography of the enzyme with confirmed predictive value have been developed: these are either 'cubic space' models[10] or mechanism-based models, and in each case are based on the outcomes of the biotransformation of a range of different ketone[11–15] and sulfide[16,17] substrates.

Currently there are no equivalent models available to predict the outcome of biooxidative transformations catalysed by Type 2 BVMOs. This is despite the demonstrated value of such enzymes, of which the best studied are 2,5-diketocamphane 1,2-monooxygenase (2,5-DKCMO) and 3,6-diketocamphane 1,6-monooxygenase (3,6-DKCMO) from camphor-grown *Pseudomonas putida* NCIMB 10007, for the production of useful chiral synthons.[18] These two diketocamphane monooxygenases are interesting enzymes since firstly they are enantiocomplementary isozymic proteins (iso-functional proteins) with their natural substrates (Fig. 1), and secondly, judged on comparative N-terminal amino acid sequence data,[1,4] they are structurally related, possibly having evolved by the accepted theory of gene duplication and subsequent divergence.[19,20]

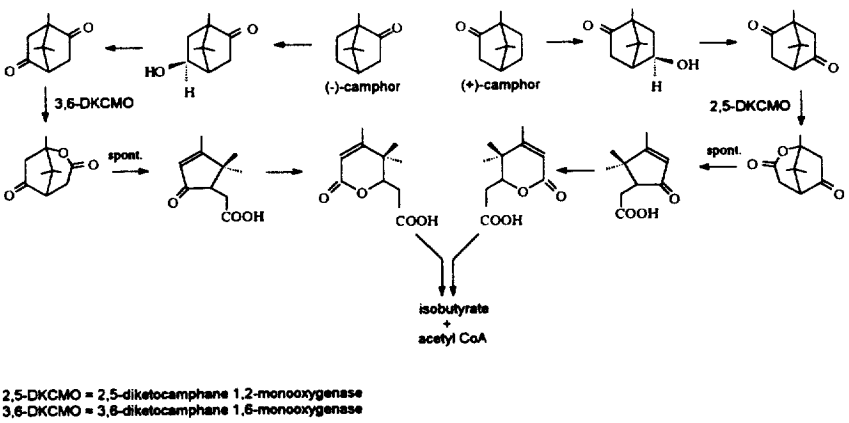

Fig. 1. The enantiocomplementary pathways of camphor metabolism in *P. putida* NCIMB 10007

The present study reports the first predictive models for chiral sulfoxidation by Type 2 BVMOs based on the analysis of the biotransformations of a substantial number of organosulfide substrates (>20) for which the absolute configuration of the resultant sulfoxides can be confirmed. There is an inherent advantage in using the outcomes of biotransformations exploiting electrophilic sulfoxidation

rather than nucleophilic lactonisation in that unlike in the case of lactone formation, the chirality of a sulfoxide product defines the stereogenic face from which the 'active oxygen' must have been delivered to the respective sulfide substrate. Models are presented for both purified isozymic diketocamphane monooxygenases isolated from camphor-grown *Pseudomonas putida* NCIMB 10007, enabling a unique comparison to be made between the active sites of two different enantiocomplementary enzymes (isozymes) believed to have evolved from a single progenitor protein. Also for the first time, this study enables comparisons to be made between active site models of both Type 1 (NADPH plus FAD-dependent) and Type 2 (NADH plus FMN-dependent) BVMOs that biotransform a similar range of organosulfide substrates.

2. Experimental approach and guidelines for 'cubic space' model building

Based on our past experience, both of BVMOs in general to perform biotransformations,[21–25] and DKCMOs in particular to biooxidise organosulfides to corresponding sulfoxides,[26] it was decided from the outset to ensure that the data processed to generate 'cubic space' models of the active site of each isozyme was internally consistent in respect of both the quality of the enzyme preparations used and the conditions under which the biotransformations were run and the products subsequently analysed. Past experience has confirmed that there is considerable batch variability in the specific activity of different enzyme preparations,[4,26] and in addition the time course for product formation has been shown to be substrate-dependent.[27]

The protocol used to produce the separate isozymes was based on that originally devised by Trudgill et al.,[28] but has been refined to yield consistently pure samples of the relevant proteins.[4,27] The known absolute enantioselective specificities of the isozymes for the respective camphor enantiomers[28] were routinely used to confirm the integrity of individual preparations (Fig. 2). In order to minimise inconsistencies in the results, a sufficient quantity of each purified isozyme to complete biooxidation of all 23 organosulfides to be tested was accumulated by pooling the relevant material prepared from a series of separate purifications conducted prior to initiating the biotransformations.

For each organosulfide substrate tested, a time course to follow both the yield and enantiomeric excess of the resultant sulfoxide product was established separately for both purified DKCMO isozymes (Fig. 3a and b). Such data enabled values to be used for subsequent model building which were considered to represent when each such biotransformation had reached a true equilibrium position. One other potentially influential factor that was assessed in each case was the subsequent biooxidation of the initial sulfoxide product(s) to an equivalent sulfone, since it is widely recognised that various microbial monooxygenases are able to catalyse the overall biotransformation of sulfides to sulfones as a sequential two-step process in which the selectivity of the second-stage enzyme-catalysed reaction can influence the relative amount of the two sulfoxides resulting from the initial biotransformation.[29] Interestingly, with both pure DKCMO isozymes, the amount, if any, of sulfone produced from all tested substrates was below detectable levels. Even when presented to either purified enzyme as the sole biotransformation substrate at both 1 mM and 10 mM, both (*S*)- and (*R*)-*p*-tolyl methyl sulfoxide yielded less than 2% of the equivalent sulfone.

Whereas some other BVMO models[14,16] have been derived from data culled from a variety of different sources with the potential inconsistencies that this approach introduces, the precautions introduced in this study were considered an essential prerequisite to validate the data used for subsequent model building of the DKCMO isozymes.

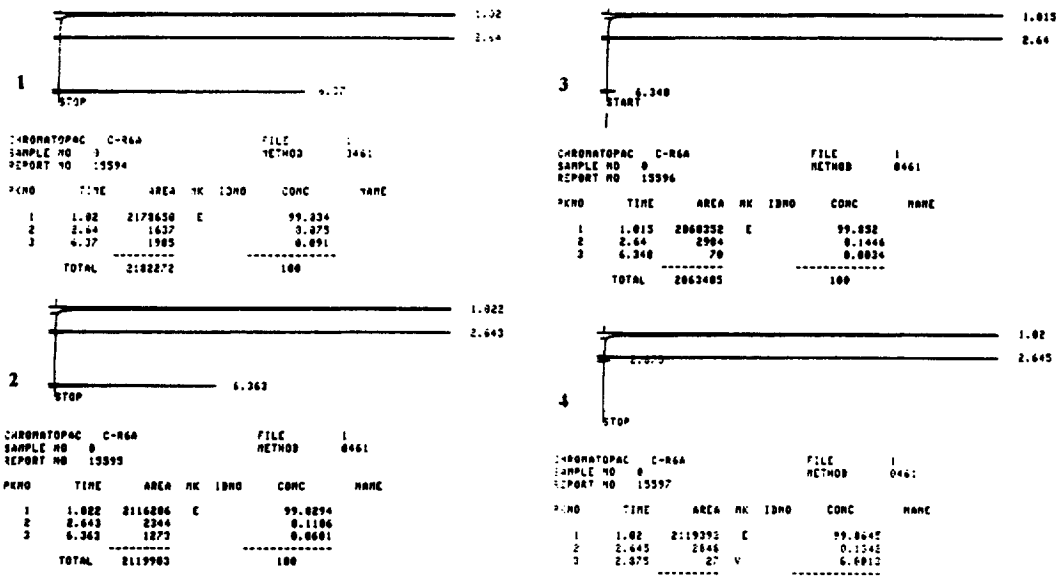

Key to GLC traces:

1. (+)-camphor substrate added to 2,5-DKCMO fraction
2. (-)-camphor substrate added to 3,6-DKCMO fraction
3. (-)-camphor substrate added to 2,5-DKCMO fraction
4. (+)-camphor substrate added to 3,6-DKCMO fraction

Elution times: (+)- and (-)-camphor: between 2.64 and 2.645 min.
equivalent lactones between 6.348 and 6.37 min.

Fig. 2. Biotransformation of (+)- and (−)-camphor by purified preparations of 2,5-DKCMO and 2,6-DKCMO

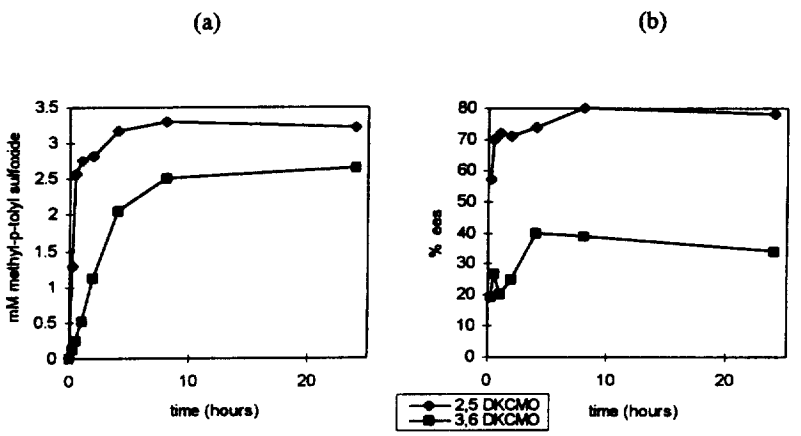

Fig. 3. Time courses of (a) yields and (b) ees of methyl-*p*-tolyl sulfoxide synthesised by DKCMO isozymes from *rac*-camphor grown *P. Putida* NCIMB 10007

3. Results and discussion

The data obtained from the biotransformation of organosulfides **1–23** (Fig. 4) by purified purifications of 2,5-DKCMO and 3,6-DCKMO are listed in Tables 1 and 2. In each case, the enantiomeric excess of the predominant sulfoxide product was established by analysis of the relevant stopped reaction mixture using either GLC (Lipodex D or Lipodex E chiral column) or HPLC (Daicel Chiracel OD chiral column),

whereas the yield was quantified by GLC (BP1 non-polar column) using a suitable internal standard. The absolute configuration of each predominant sulfoxide product was established by comparison of GC or HPLC traces with those of authentic standards of known configuration assayed under identical conditions.

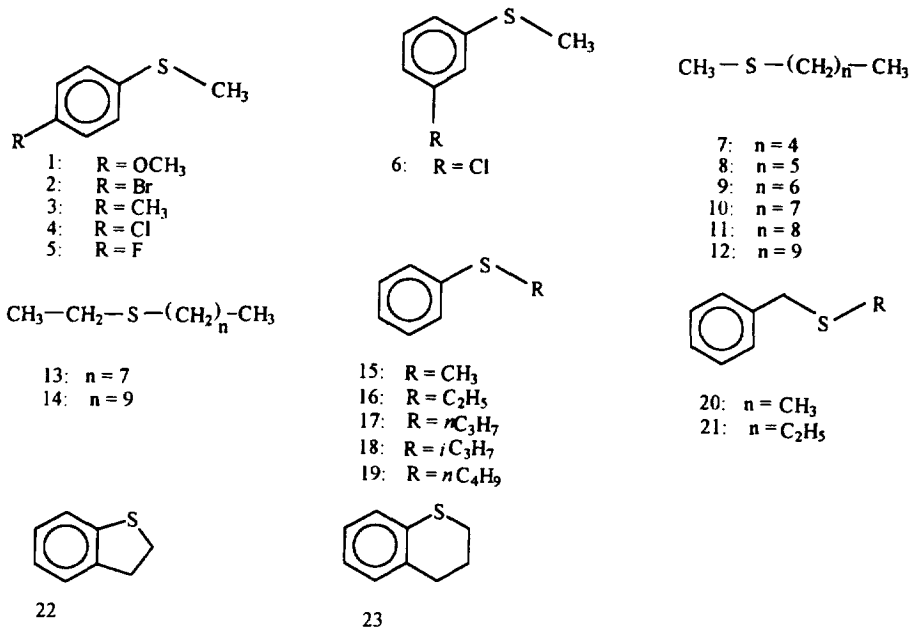

Fig. 4. Organosulfides biotransformed by 2,5-DKCMO and 3,6-DKCMO

The results revealed some significant differences in the pattern of biooxidations catalysed by the two purified DKCMO isozymes. Although the chemoselectivity of both enzymes was similar as reflected by the range of tested substrates able to serve as competent substrates, 2,5-DKCMO typically oxidised equivalent sulfides with lower yields of the respective sulfoxides. Interestingly, in contrast, higher yields of lactones were synthesised from respective ketone substrates by 2,5-DKCMO.[4,25] This may reflect (a) difference(s) in the structural relationship in the two isozymes between the apoprotein and the essential FMN cofactor that serves in each case as the vehicle for delivering 'active oxygen'; in this respect it may be significant that the role of the FMN cofactor is different in electrophilic and nucleophilic biooxidation.[30]

With a few notable exceptions of which the best examples are $C_6H_5S^nC_4H_9$ and $C_6H_5S^nC_3H_7$, the enantioselectivity of 2,5-DKCMO was higher than 3,6-DKCMO for equivalent biooxidations, although this discrepancy was substrate-dependent. This is consistent with the relative performance of the two isozymes in catalysing the nucleophilic oxygenation of various bicyclic ketones.[4,25] As a general trend, *para*-substitution of the aromatic ring of alkyl aryl sulfides had a significant (*S*)-directing influence on the outcome of events in the active sites of both isozymes with the notable exception of *p*-fluorophenyl methyl sulfide which, although oxidised to the equivalent (*S*)-sulfoxide by 2,5-DKCMO as expected from the preceding generalisation, was oxidised to the antipodal oxide by 3,6-DKCMO. Significantly, both biooxidations occurred with considerable enantioselectivity, suggesting enantiocomplementary accommodation of this particular substrate in the active sites of the two isozymes. The alkyl chain of the unsubstituted *n*-alkyl aryl sulfides also had a noticeable effect; with 2,5-DKCMO, lengthening the chain in the homologous series from methyl to *n*-butyl resulted in a progressively (*R*)-directing effect, whereas with 3,6-DKCMO no such trend was detectable. The branched-chain alkyl aryl sulfide $C_6H_5S^iC_3H_7$ was another interesting substrate; as like $pFC_6H_4SCH_3$, it exposed a significant difference

Table 1
The biotransformation of organosulfides **1–23**: numerical sequence

	2,5-DIKETOCAMPHANE 1,2-MONOOXYGENASE			3,6-DIKETOCAMPHANE 1,6-MONOOXYGENASE		
SULFIDES OXIDISED	**GLC yield**	**ee**	**Config.***	**GLC yield**	**ee**	**Config.***
$pCH_3OC_6H_4SCH_3$ **1**	29%	71%	(*S*)	65%	25%	(*S*)
$pBrC_6H_4SCH_3$ **2**	2%	56%	(*S*)	13%	50%	(*S*)
$pCH_3C_6H_4SCH_3$ **3**	12%	62%	(*S*)	57%	32%	(*S*)
$pClC_6H_4SCH_3$ **4**	5%	45%	(*S*)	15%	27%	(*S*)
$pFC_6H_4SCH_3$ **5**	9%	39%	(*S*)	72%	30%	(*R*)
$mClC_6H_4SCH_3$ **6**	6%	48%	(*S*)	29%	22%	(*S*)
$CH_3S(CH_2)_4CH_3$ **7**	28%	32%	(*S*)	90%	0	*racemic*
$CH_3S(CH_2)_5CH_3$ **8**	19%	37%	(*S*)	50%	19%	(*S*)
$CH_3S(CH_2)_6CH_3$ **9**	10%	30%	(*S*)	43%	20%	(*S*)
$CH_3S(CH_2)_7CH_3$ **10**	6%	36%	(*S*)	20%	16%	(*S*)
$CH_3S(CH_2)_8CH_3$ **11**	1.6%	16%	(*S*)	9%	8%	(*R*)
$CH_3S(CH_2)_9CH_3$ **12**	1.1%	5%	(*S*)	6%	9%	(*R*)
$C_2H_5S(CH_2)_7CH_3$ **13**	3%	21%	(*S*)	14%	14%	(*S*)
$C_2H_5S(CH_2)_9CH_3$ **14**	0.5%	4%	(*S*)	1.2%	11%	(*R*)
$C_6H_5SCH_3$ **15**	9%	35%	(*S*)	53%	9%	(*S*)
$C_6H_5SC_2H_5$ **16**	5%	2%	(*R*)	25%	0	*racemic*
$C_6H_5SnC_3H_7$ **17**	8%	8%	(*R*)	20%	19%	(*S*)
$C_6H_5SiC_3H_7$ **18**	11%	20%	(*S*)	21%	24%	(*R*)
$C_6H_5SnC_4H_9$ **19**	5%	11%	(*R*)	14%	43%	(*S*)
$C_6H_5CH_2SCH_3$ **20**	29%	30%	(*S*)	85%	4%	(*R*)
$C_6H_5CH_2SC_2H_5$ **21**	20%	2%	(*S*)	41%	9%	(*R*)
$C_6H_4S(CH_2)_2$ **22** 2,3-dihydrobenzothiophene	18%	38%	(*S*)	24%	41%	(*R*)
$C_6H_4S(CH_2)_3$ **23** 1-thiatetrahydronapthalene	15%	17%	(*S*)	28%	7%	(*R*)

between the two isozymes, being oxidised predominantly to the (*S*)-sulfoxide by 2,5-DKCMO but its complementary enantiomer by 3,6-DKCMO. Similarly, both tested alkyl benzyl sulfides ($C_6H_5CH_2SCH_3$ and $C_6H_5CH_2SC_2H_5$) were oxidised with similar, but opposite, enantioselectivities to the corresponding (*S*)- and (*R*)-sulfoxides by 2,5-DKCMO and 3,6-DKCMO respectively.

The dialkyl sulfides, although they have the disadvantage of conformational flexibility, were used as substrates to attempt to define the limits of the active site topography of both DKCMO isozymes. No detectable products were recorded when $CH_3S^nC_3H_7$ and $CH_3S^nC_4H_9$ were presented to either isozyme, possibly because the high volatility of the compounds reduced their effective concentration in the biotransformation mixture below a threshold at which either enzyme-catalysed biooxidation could occur or the resultant sulfoxide products could be detected. Higher homologues up to and including

Table 2
The biotransformation of organosulfides **1–23**: data from Table 1 ranked by enantioselectivity

2,5-DIKETOCAMPHANE 1,2-MONOOXYGENASE			3,6-DIKETOCAMPHANE 1,6-MONOOXYGENASE		
SULFIDES OXIDISED	ee	config.	config.	ee	SULFIDES OXIDISED
1 $pCH_3OC_6H_4SCH_3$	71%	(*S*)	(*S*)	50%	$pBrC_6H_4SCH_3$ 2
3 $pCH_3C_6H_4SCH_3$	62%	(*S*)	(*S*)	43%	$C_6H_5SnC_4H_9$ 19
2 $pBrC_6H_4SCH_3$	56%	(*S*)	(*S*)	32%	$pCH_3C_6H_4SCH_3$ 3
6 $mClC_6H_4SCH_3$	48%	(*S*)	(*S*)	27%	$pClC_6H_4SCH_3$ 4
4 $pClC_6H_4SCH_3$	45%	(*S*)	(*S*)	25%	$pCH_3OC_6H_4SCH_3$ 1
5 $pFC_6H_4SCH_3$	39%	(*S*)	(*S*)	22%	$mClC_6H_4SCH_3$ 6
22 $C_6H_4S(CH_2)_2$ 2,3-dihydrobenzothiophene	38%	(*S*)	(*S*)	20%	$CH_3S(CH_2)_6CH_3$ 9
8 $CH_3S(CH_2)_5CH_3$	37%	(*S*)	(*S*)	19%	$CH_3S(CH_2)_5CH_3$ 8
10 $CH_3S(CH_2)_7CH_3$	36%	(*S*)	(*S*)	19%	$C_6H_5SnC_3H_7$ 17
15 $C_6H_5SCH_3$	35%	(*S*)	(*S*)	16%	$CH_3S(CH_2)_7CH_3$ 10
7 $CH_3S(CH_2)_4CH_3$	32%	(*S*)	(*S*)	14%	$C_2H_5S(CH_2)_7CH_3$ 13
9 $CH_3S(CH_2)_6CH_3$	30%	(*S*)	(*S*)	9%	$C_6H_5SCH_3$ 15
20 $C_6H_5CH_2SCH_3$	30%	(*S*)	*racemic*	0	$CH_3S(CH_2)_4CH_3$ 7
13 $C_2H_5S(CH_2)_7CH_3$	21%	(*S*)	*racemic*	0	$C_6H_5SC_2H_5$ 16
18 $C_6H_5SiC_3H_7$	20%	(*S*)	(*R*)	4%	$C_6H_5CH_2SCH_3$ 20
23 $C_6H_4S(CH_2)_3$ 1-thiatetrahydronapthalene	17%	(*S*)	(*R*)	7%	$C_6H_4S(CH_2)_3$ 23 1-thiatetrahydronapthalene
11 $CH_3S(CH_2)_8CH_3$	16%	(*S*)	(*R*)	8%	$CH_3S(CH_2)_8CH_3$ 11
12 $CH_3S(CH_2)_9CH_3$	5%	(*S*)	(*R*)	9%	$CH_3S(CH_2)_9CH_3$ 12
14 $C_2H_5S(CH_2)_9CH_3$	4%	(*S*)	(*R*)	9%	$C_6H_5CH_2SC_2H_5$ 21
21 $C_6H_5CH_2SC_2H_5$	2%	(*S*)	(*R*)	11%	$C_2H_5S(CH_2)_9CH_3$ 14
16 $C_6H_5SC_2H_5$	2%	(*R*)	(*R*)	24%	$C_6H_5SiC_3H_7$ 18
17 $C_6H_5SnC_3H_7$	8%	(*R*)	(*R*)	30%	$pFC_6H_4SCH_3$ 5
19 $C_6H_5SnC_4H_9$	11%	(*R*)	(*R*)	41%	$C_6H_4S(CH_2)_2$ 22 2,3-dihydrobenzothiophene

$CH_3S^nC_8H_{17}$ were oxidised in relatively good yields to (*S*)-sulfoxides with moderate ees by 2,5-DKCMO whereas in accordance with the general trend, these same substrates were oxidised with lower enantioselectivity by 3,6-DKCMO to the extent that $CH_3S^nC_5H_{11}$ yielded the racemic oxide product. Higher homologues in this series yielded significantly decreased amounts of the equivalent sulfoxides, possibly because the solubility threshold of these particular substrates reduced their effective availability for biooxidation, with 2,5-DKCMO yielding products with a low (*S*)-, and 3,6-DKCMO a low (*R*)-predominance.

The bicyclic sulfides 2,3-dihydrobenzothiophene and 1-thiatetrahydronaphthalene were considered to be of particular value to the modelling studies because of their relative conformational stability.

Interestingly, these two sulfides were oxidised in an enantiocomplementary way by the two isozymes, with 2,5-DKCMO yielding predominantly (*S*)-sulfoxides and 3,6-DKCMO the equivalent (*R*)-antipodes.

The catalogue of information on the stereoselectivity of the biooxidation of the various thioethers by the two purified DKCMO isozymes was computed into 'cubic space' models depicting the binding pockets of the respective active sites.[10] Initially, the total energy of each separate sulfoxide product was minimised (MM^+) using the molecular modelling programme HyperChem® (release 5):[31] in each case, the atoms were considered in point form and the relevant hydrogen atoms were included. Considering each isozyme separately, the sulfoxide products were then initially grouped according to the recorded absolute configuration of the predominant metabolite: racemic sulfoxides (<5% ee) were included in both groups. For each resultant group, particular combinations of minimised structures of the relevant sulfoxide products, chosen on grounds of chemical relatedness, were overlaid by prior precedent[16] along the O=S–C axis and centred at the S atom. The chosen C–S bond of the phenyl and benzyl alkyl sulfides links the heteroatom to the aryl moiety of these compounds, whereas the defined C–S bond used in the case of the dialkyl sulfides is the one that tethers the longer alkyl side chain. The chosen combinations of overlaid sulfoxides and the progressive way in which these groups were themselves superimposed are shown in Figs 5 and 6 which includes illustrative examples of the resultant outcomes: the 'stick' rendering of the minimised sulfoxide structures was necessary for taking molecular measurements to aid model building (*vide supra*), whereas the 'ball' rendering of the same molecules was used to gain a better grasp of the space-filling dimensions.

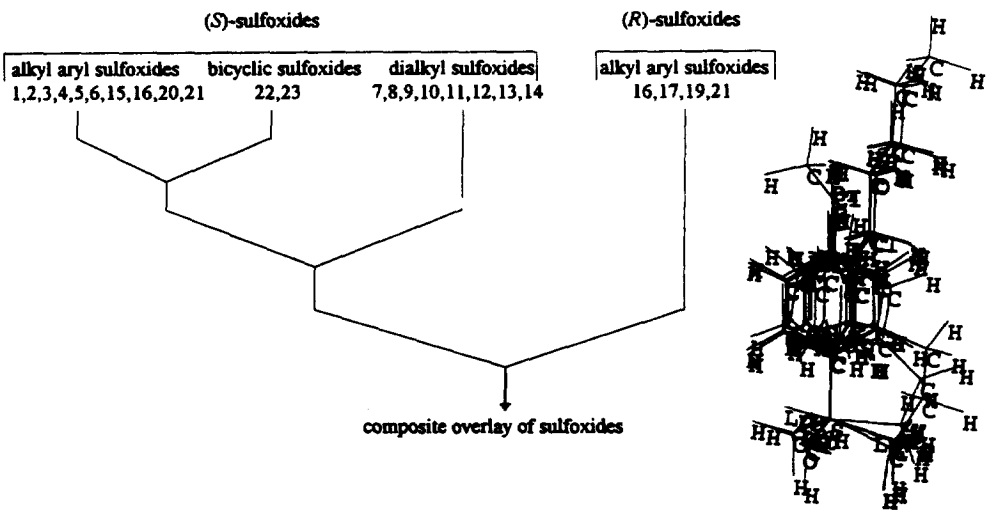

Fig. 5. Rationale for superimposing the minimised structures of the sulfoxides formed by 2,5-DKCMO

For each separate purified DKCMO isozyme, the three-dimensional picture which emerged based on the outcomes of sulfide biotransformations catalysed by that particular enzyme can be used to delineate an image of the confines of the active site within which the relevant oxygenations took place. Because the molecules used to define these models are hydrophobic, in the majority of cases consisting of a sulfur atom substituted with both a relatively large and a relatively small hydrophobic group, and because each isozyme yielded examples of both (*S*)- and (*R*)-series sulfoxides, each active site model was constructed to contain four discrete, albeit arbitrarily defined, hydrophobic pockets (H_1–H_4).

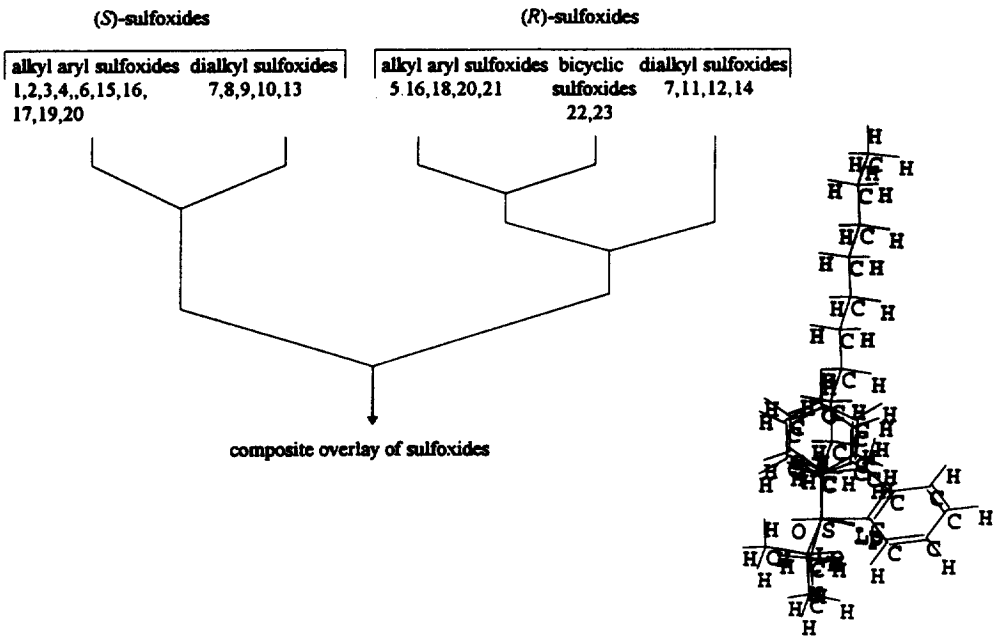

Fig. 6. Rationale for superimposing the minimised structures of the sulfoxides formed by 3,6-DKCMO

3.1. *Large hydrophobic pocket H_1*

The superimposed (*S*)-alkyl aryl and (*S*)-dialkyl sulfoxides were used to define the H_1 hydrophobic pocket which was deemed to contain the aryl moieties (H_{1a} subdomain) and the larger of the alkyl groups (H_{1b} subdomain) respectively. It was assumed that there was an anchoring site for the *para*-substituted groups of the aryl rings at one extremity of the H_{1a} subdomain. For the purposes of establishing the 'depth' of the H_{1a} and H_{2a} subdomains, in each case measurements were made from the sulfur atom to either the most distal substituent at the *para*- or *meta*-position of the phenyl ring, or the terminal proton of the longer alkyl side chain as appropriate. To help define further the topography of the pocket, the distances across the aromatic rings (hydrogen atom to hydrogen/halogen atom) and the alkyl chains (hydrogen atom to hydrogen atom) were calculated for each sulfoxide, and then used to define the remaining dimensions of the H_{1a} and H_{1b} subdomains respectively, assuming in each case that the sulfur atom was located centrally in the 'base' at one of the distal ends. In establishing the dimensions of the H_{1b} subdomain, the alkyl groups were each modelled in as the extended conformer in order to represent one possible extreme of demand for 'cubic space' of these groups in that part of the active site: because of the way that the individual subdomains are subsequently superimposed in devising the active site models (*vide supra*), the alternative conformers of these alkyl sidechains can be accomodated within the dimensions of the H_{1a} subdomain.

Also included were the aryl moieties of the (*S*)-sulfoxide products resulting from the biotransformation of the two tested bicyclic organosulfides (**22** and **23**). The equivalent heterocyclic rings were found to occupy a discrete subdomain of the pocket (H_{1c}) which was modelled to take into account the restricted conformational mobility of the bicyclic sulfide substrates. It was apparent that while H_{1c} predominantly coincided with the H_{1a} subdomain, it also impinged into the equivalent small hydrophobic pockets H_3 and H_4 (*vide supra*), thereby helping to define the interface between these various domains of 'cubic space'.

3.2. Large hydrophobic space H_2

The corresponding subdomains H_{2a}, H_{2b} and H_{2c} were modelled and equivalent measurements made as for H_1, but in this case defined by overlaying sulfoxides of (*R*)-configuration. Again, the H_{2c} subdomain assumed particular significance but unlike in the H_1 pocket, the H_{2c} and H_{2a} subdomains did not coincide, thereby occupying a greater area of 'cubic space'. However, the H_{2c} like the H_{1c} subdomain did overlap to some extent with both the H_3 and H_4 small hydrophobic pockets thereby helping to define the relationship between these different domains of 'cubic space'.

3.3. Small hydrophobic pocket H_3

The H_3 pocket was defined by making equivalent measurements of the alkyl chains of the superimposed alkyl aryl sulfoxides with aromatic rings occupying the H_1 pocket. The dimensions of the shorter alkyl chains of the superimposed dialkyl sulfoxides with the longer alkyl chains occupying the H_1 pocket were also included to establish the dimensions of this pocket.

3.4. Small hydrophobic pocket H_4

Equivalent measurements were made as for H_3, but in this case defined by overlaying sulfoxides of (*R*)-configuration.

The resultant pockets so defined for the 2,5-DKCMO and 3,6-DKCMO isozymes purified from *Pseudomonas putida* NCIMB 10007 are shown separately in Figs 7 and 8 respectively. However, the real boundaries of the four binding pockets probably remain to be established as the current dimensions can only reflect the outcomes of sulfide substrates tested in the present study: the actual boundaries might well extend beyond those presently charted.

Finally, for each purified protein, the four separate binding pockets were superimposed using the same general principles employed in developing other sulfoxidation-based models.[14,16,32] Using the S atom as a focal point and taking into account the bond angles emanating from this centre, (H_1+H_3) and (H_2+H_4) were aligned along the S=O axis to define the total dimensions in 'cubic space' terms of the active site of both the DKCMO isozymes responsible for the electrophilic biooxidation of the tested range of organosulfides [Fig. 9(a) and (b)].

While this approach to modelling the active sites of the two DKCMO isozymes is similar to that used to visualise the active site of CHMO from *A. calcoaceticus* NCIMB 9871,[14,16] the 'cubic space' models are likely to be a more accurate representation because of the higher quality of the computed data used (*vide infra*). The DKCMO isozyme models are also more advanced in that the CHMO model defines just three active site regions (pockets), hydrophobic large (H_L=H_1), hydrophobic small (H_S=H_4), and a large poorly defined main region (M) corresponding to the combined H_2 and H_3 pockets of the current models. Interestingly, both DKCMO isozyme models share some structural features with the model developed to rationalise >90 organosulfide biotransformations catalysed by whole-cell preparations of *Helminthosporium* sp. NRRL 4671.[32] All three models propose the occurrence of a large hydrophobic pocket containing a strategic distal anchoring site (DKCMO models=coincident regions of the H_1 plus H_2 domains, NRRL 4671=PHP) and two smaller adjacent hydrophobic pockets (DKCMO models=H_3 and H_4 domains, NRRL 4671=H_S and H_L). While it has to be appreciated that the pattern of biooxidations used to complete the model for *Helminthosporium* sp. NRRL 4671 may result from the combined activity of two or more separate enzymes in the whole-cell preparations, it is significant that active site models that contain two or more spacially defined hydrophobic binding regions with a polar binding

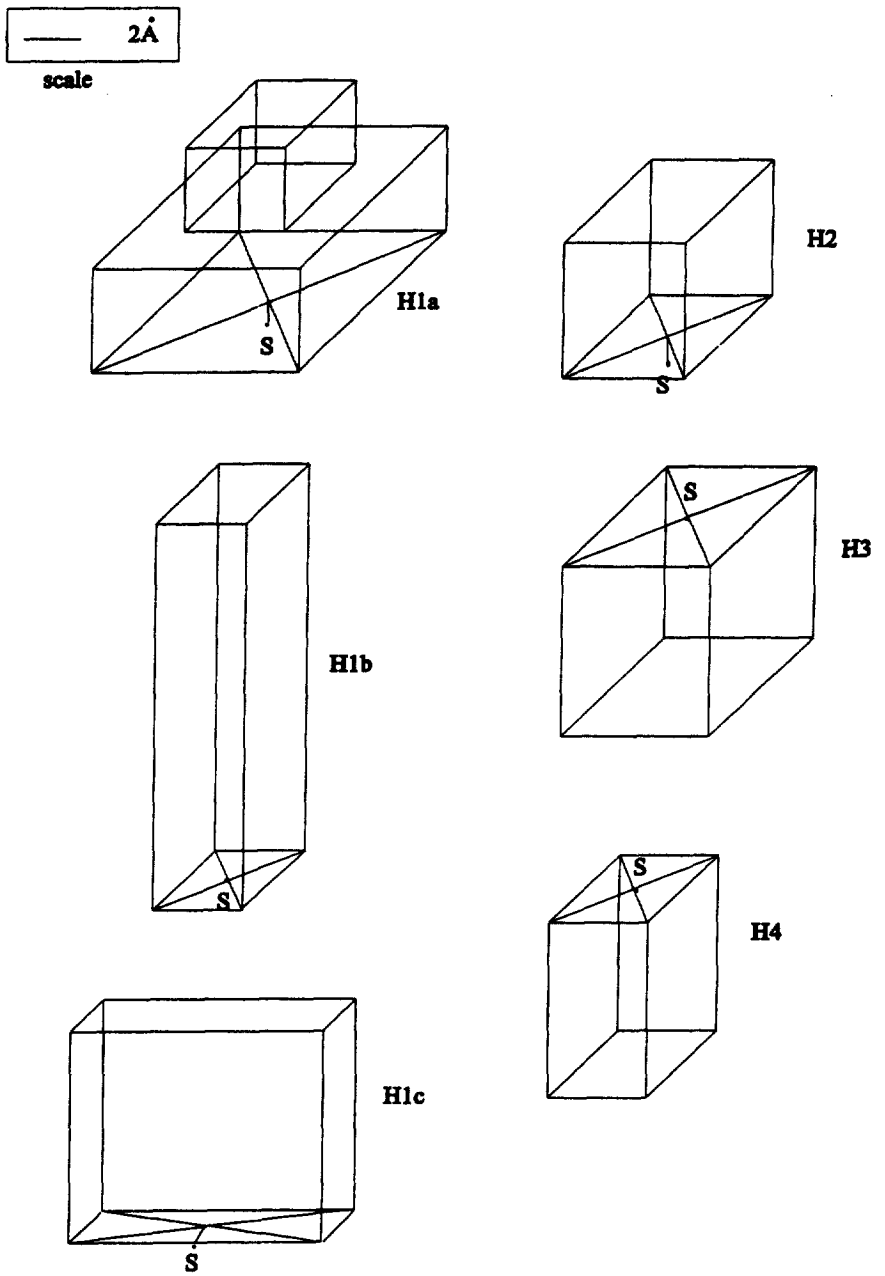

Fig. 7. Dimensions of active side pockets of 2,5-DKCMO estimated from sulfoxide overlay measurements

site are common to other oxidative enzymes of known (cytochrome $P450_{cam}$ MO)[33–35] and unknown (CHMO)[14,16] structure.

Clearly there are limitations on the interpretations of these data used to obtain the first models of the active sites of Type 2 Baeyer–Villiger monooxygenases. Firstly, the calculated measurements of the dimensions of the active site pockets are, of necessity, minimum dimensions resulting from the nature of the sulfide substrates tested to date. Secondly, no allowance has been made for electronic effects resulting from the chemical nature of the substrates used: it is known that electronic as well as stereochemical

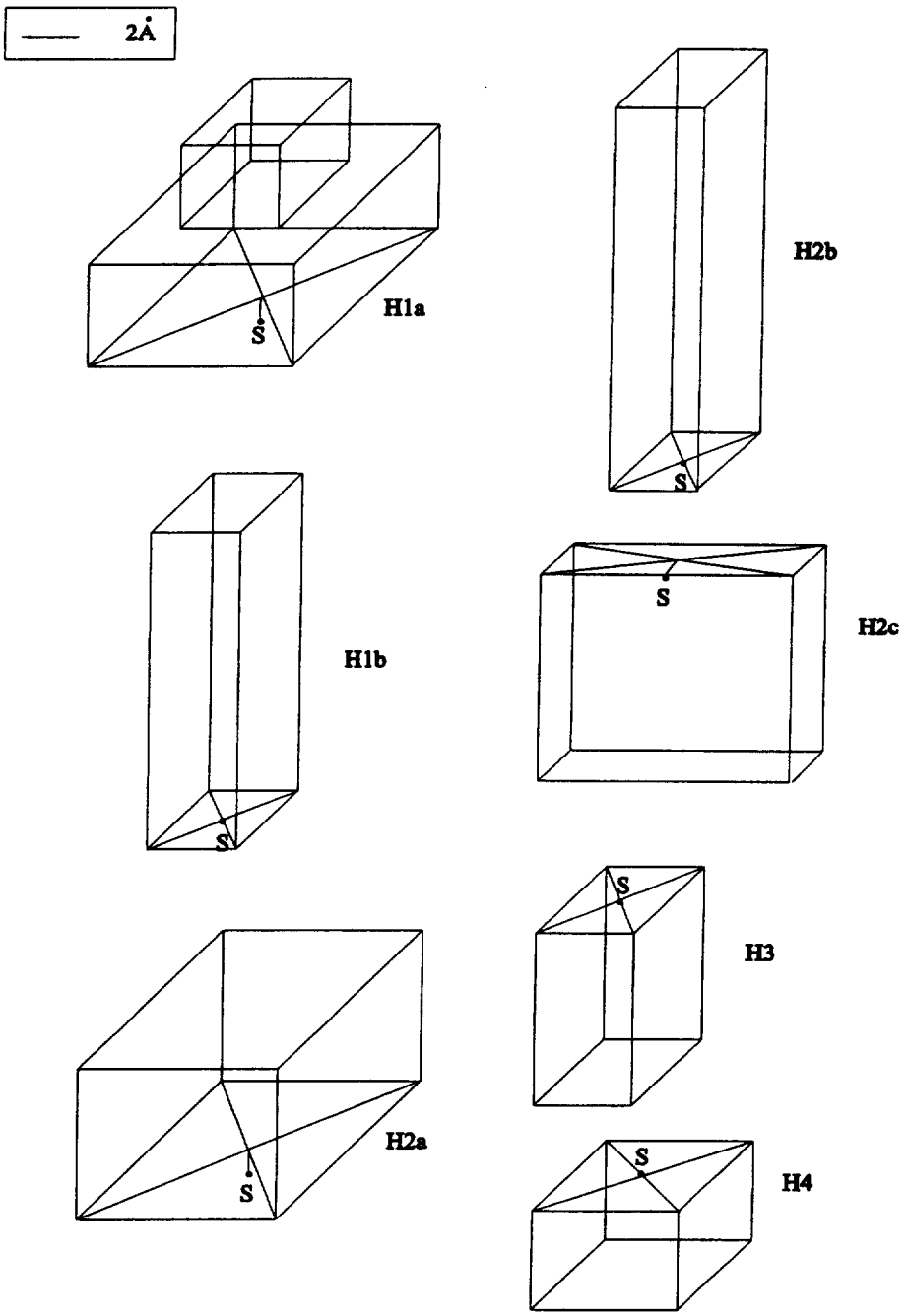

Fig. 8. Dimensions of active side pockets of 3,6-DKCMO estimated from sulfoxide overlay measurements

effects contribute to the outcome of many enzyme-catalysed reactions, including those catalysed by Baeyer–Villiger monooxygenases.[36,37] Thirdly, because of the limited database so far available, the proposed models only apply to the biotransformation of hydrophobic compounds such as thioethers.

The outcomes from the 23 competent sulfide substrates used to construct the models do indicate that the equivalent H_1 binding pockets (large hydrophobic groups of (*S*)-sulfoxides) of both the 2,5-DKCMO

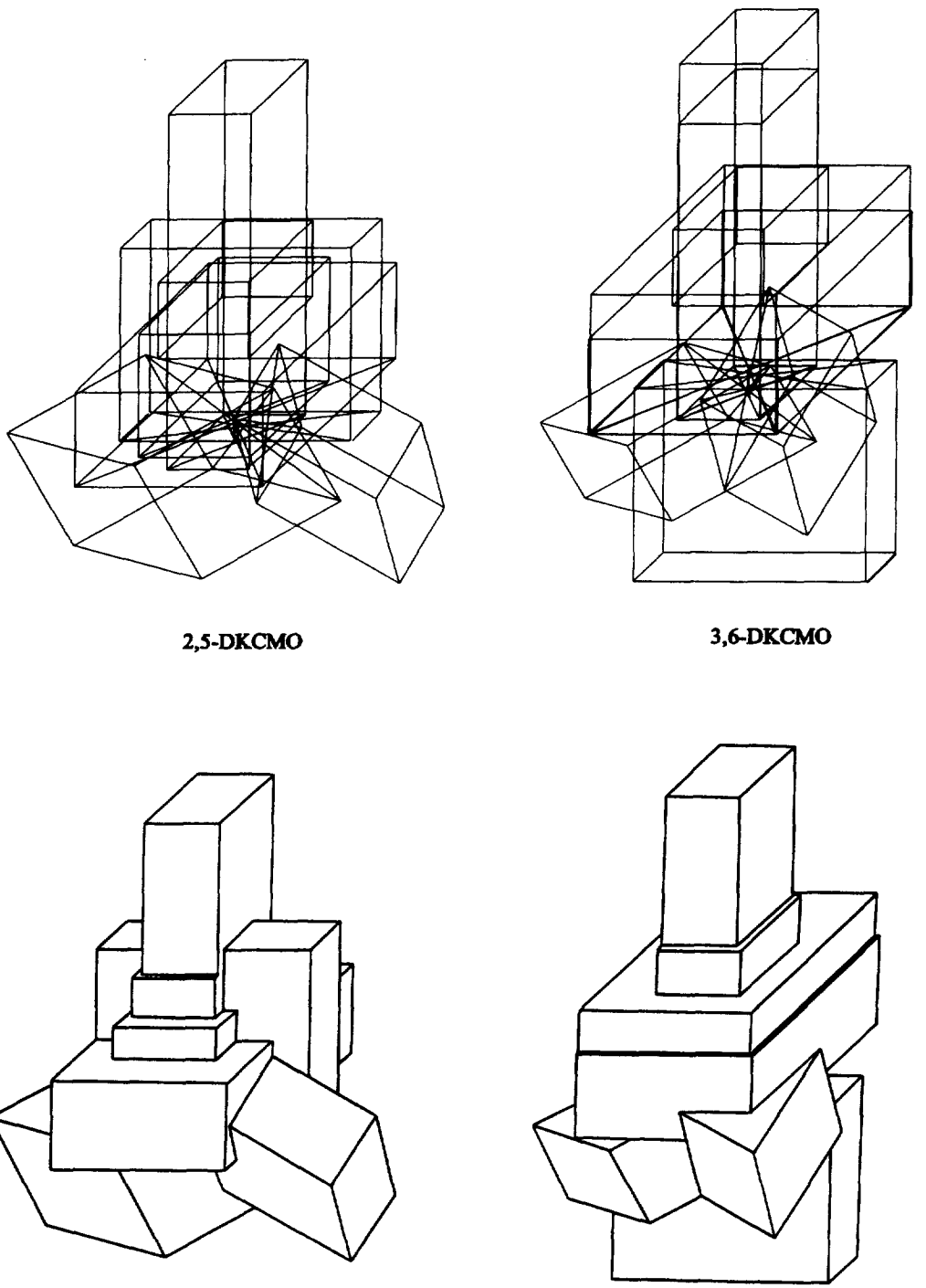

Fig. 9. (a) Overall impression of the total dimension ('cubic space') of the active sites of 2,5-DKCMO and 3,6-DKCMO; (b) three-dimensional projections of the 'cubic space' active site models of 2,5-DKCMO and 3,6-DKCMO abstracted from the data shown in (a)

and 3,6-DKCMO isozymes were similar. In each case, the H_{1a} subdomain was extensive enough to be able to accommodate both a chlorine atom in the *meta*-position and various substituents (CH_3O-, CH_3-, Br-, Cl-) in the *para*-position on the phenyl ring of various substrates. The extended conformers of the longer chain alkyl groups up to the octyl homologue would be able to fit into both H_{1b} subdomains, while because of the way that the subdomains have been superimposed, the alternative conformers of these alkyl sidechains would be accomodated within the dimensions of the extensive H_{1a} subdomains. A feature of active site models of both DKCMO isozymes was that because of the relative orientations assumed by the aryl rings and the longer chain alkyl groups, there was no apparent conflict between the requirement within the same subdomain for active site environments compatible with accomodating both the hydrophobic hydrocarbon chains and the more polar aryl substituents. One notable difference was the necessity to accommodate the (*S*)-sulfoxide products of the two bicyclic substrates tested in a separate H_{1c} subdomain of the active site of 2,5-DKCMO only.

Definition of the dimensions of the H_2 binding pocket (large hydrophobic groups of (*R*)-sulfoxides) of 2,5-DKCMO was problematical because of the paucity of relevant products: the only relevant subdomain that could be modelled was H_{2a} to accommodate the phenyl ring of a small number of alkyl aryl sulfoxides. With 3,6-DKCMO, however, the 'cubic space' could be defined with much greater confidence and precision because of the need to accommodate the predominantly (*R*)-sulfoxides resulting from the biooxidation of various alkyl aryl- (H_{2a}), dialkyl- (H_{2b}) and bicyclic (H_{2c}) sulfides. Overall, on the basis of the outcomes of the biotransformations characterised to date, the dimensions of the H_2 binding pocket of 3,6-DKCMO were substantially bigger than the equivalent 'cubic space' of 2,5-DKCMO, particularly in view of the orientation of the H_{2c} subdomain relative to H_{2a} and H_{2b}. One particularly interesting substrate in this respect was *p*-fluorophenyl methyl sulfide: although 2,5-DKCMO oxidised this substrate to the (*S*)-sulfoxide in common with other *para*-substituted alkyl aryl sulfides indicating in each case that the relevant aryl moiety was accommodated in the H_{1a} subdomain, 3,6-DKCMO oxidised this same substrate in a substantially higher yield to predominantly the opposite antipode. One possible explanation is that this exception may reflect a size constriction within the binding site at the distal end of the H_{2a} binding pocket of 3,6-DKCMO which allows access of the *p*-fluorophenyl methyl sulfide to the exclusion of other *para*-substituted homologues.

When compared, the dimensions of both the H_3 and H_4 small hydrophobic binding pockets also showed some differences between the two DKCMO isozymes, and interestingly these reflected themselves in an enantiocomplementary way. Thus the comparatively greater dimensions of the 'cubic space' occupied by the H_3 domain of 2,5-DKCMO was matched by a disproportionately greater 'cubic space' for the H_4 domain of the 3,6-DKCMO isozyme.

The total 'cubic space' occupied by the modelled active sites of both DKCMO isozymes was similar (approximately 750–900 $Å^3$. This would suggest that the active sites of these Type 2 BVMOs may be up to 30% larger than that of CHMO, the Type 1 BVMO from *A. calcoaceticus* NCIMB 9871.[14] This discrepancy may reflect the fact that whereas the hexyl group was the largest alkyl chain modelled into the CHMO active site, the current models were devised to accommodate alkyl chains up to the decyl group.

Overall, the study has demonstrated both some similarities and some significant differences between the active site domains of the two DKCMO isozymes from *rac*-camphor grown *Pseudomonas putida* NCIMB 10007. The typically lower enantioselectivity observed for biooxidations catalysed by 3,6-DKCMO compared with 2,5-DKCMO with a wide range of both sulfide (this study) and ketone substrates[24,25] equates with the overall greater dimensions of the active site of the former enzyme. From this analysis, both the H_2 pocket (large hydrophobic groups of (*R*)-sulfoxides), most notably the H_{2b} and H_{2c} subdomains, and the H_4 hydrophobic pocket (small hydrophobic groups of (*R*)-sulfoxides)

of 3,6-DKCMO are substantially larger than the equivalent 'cubic space' in the active site of the 2,5-DKCMO isozyme. This is illustrated by a comparison of the relevant data in Tables 1 and 2 which showed that for the 23 tested sulfides, 2,5-DKCMO yielded 82% (*S*)-sulfoxides, 9% (*R*)-sulfoxides and 9% (*rac*)-sulfoxides, whereas 3,6-DKCMO yielded 52% (*S*)-sulfoxides, 35% (*R*)-sulfoxides and 13% (*rac*)-sulfoxides.

The study has not only emphasised that both DKCMO isozymes have broad chemospecificity with regard to the range of organosulfides that can be biooxidised, but has also served to highlight classes of sulfide substrates which could be tested to seek data to further define the dimensions of the active site pockets more accurately. Thus conformationally rigid bicyclic sulfides and disulfides both with and without substituents, alkyl aryl sulfides with *ortho*- and/or *meta*-ring substituents, dialkyl sulfides containing at least one branched and/or unsaturated alkyl chain, and benzyl sulfides have either demonstrated their value or their potential for further study has been recognised.

The empirical approach that has been adapted to mapping the topography of the active site of the two Type 2 Baeyer–Villiger monooxygenase isozymes has a number of advantages. Firstly, the relative simplicity of the experimental data required compared to the alternative approach based on the assumption that suitable crystalline forms of these proteins can be obtained that produce sufficient quality and quantity of X-ray diffraction data, allied to knowledge of the respective full amino acid sequence data, has considerably shortened the time-scale involved. Secondly, the 'cubic space' representations of the active sites are dynamic mode-of-action models derived from real kinetic data that in each case reflect the enzymic mechanism of each protein. This is in strict contrast to X-ray diffraction data which can only give a static representation of one form of the protein, albeit that of the complete molecule rather than just the active site, often crystallised out under conditions totally alien to those in which the enzyme would normally function. A related issue is that the models obtained reflect the outcome of the dynamic interaction of both types of protein subunits (oxygenating subunit and NADH dehydrogenase) in these Type 2 Baeyer–Villiger monooxygenases, whereas X-ray diffraction data obtained from crystals of a pure oxygenating subunit or pure NADH dehydrogenase would not reflect the recognised integrated functionality of these two distinct oligopeptides.[28,38] A further advantage of this 'cubic space' modelling approach is that it has value for both the explanation and prediction of the stereoselectivities of the DKCMO isozymes but, in common with the alternative approach, it does suffer from the limitation of being incapable of making predictions about either the expected yield(s) of product(s) or relevant kinetic parameters such as K_m and V_{max}.

Finally, the study is unique in providing an insight into the structural relationship of the active sites of two proteins from the same living organism that have evolved to exhibit enantiocomplementary stereoselectivity with their respective natural substrates (Fig. 1). These two DKCMO isozymes are known to show considerable sequence homology from the limited sequence data available.[1,4] The natural evolution of novel enzyme activities is widely accepted to involve duplication of an existing gene followed by mutation resulting in divergence of substrate specificity.[19,20] If the initial form of the enzyme were able to accept one enantiomer of the natural substrate only, it is possible that this form, when duplicated, then evolved to change its enantiomeric preference, possibly as a result of expansion of one or more subdomains of the active site, thereby implicating the evolutionary relationship of the two DKCMO isozymes induced by growth of *Pseudomonas putida* NCIMB 10007 on *rac*-camphor.

4. Experimental

4.1. Apparatus, materials and methods

Analyses by GLC were performed using Shimadzu GC 14A machines fitted with Lipodex D and Lipodex E chiral resolution columns. Equivalent chemically synthesised racemic standards were used to characterise the behaviour of particular sulfoxides on the columns and establish the elution times of complementary enantiomers. Analyses by ^{1}H NMR were made at 300 MHz (Bruker AM-300) in the presence of Eu(hfc)$_3$ as the chiral shift reagent.

Absolute configurations of sulfoxides were determined in one or more different ways as appropriate. Where possible, the GLC elution times of chemically synthesised samples of homochiral enantiomers of confirmed configuration were compared with those of biogenic origin. In some cases, optical rotations were determined and compared with those reported in the literature for equivalent authentic samples: in each case the samples were made up in the same solvent specified in the literature and read at 20°C using an AA1000 Optical Activity polarimeter.

4.2. Maintenance of microorganisms

Pseudomonas putida NCIMB 10007 (ATCC 17435) was obtained from the National Collection of Industrial and Marine Bacteria, Aberdeen, Scotland and maintained on nutrient agar slopes at 28°C. The organism was routinely grown on a basal salts medium: NH_4Cl (2 g), K_2HPO_4 (8.2 g), KH_2PO_4 (3.1 g), yeast extract (0.1 g) and tryptone (0.1 g). $MgSO_4 \cdot 7H_2O$ (0.4 g), $MnSO_4 \cdot H_2O$ (0.05 g), $CaCl_2 \cdot H_2O$ (0.01 g) and $NaMoO_4$ (0.01 g) were added prior to autoclaving the medium at 15 psi for 15 min and then $FeSO_4 \cdot 7H_2O$ (0.05 g L^{-1}) and *rac*-camphor (2.5 g L^{-1}) were added. A 100 ml culture of the bacterium was inoculated from a stock slope and after 24 h growth at 28°C on an orbital incubator (150 rpm) was transferred to 1 L of the same medium. After a further 24 h of growth this culture was used to inoculate 10 L of sterile medium in a 20 L glass fermenter which was sparged with sterile air at 4 L^3 min^{-1}. Growth of the bacterium was monitored by transferring 1 ml aliquots of a growing cell suspension to a plastic cuvette and reading the absorbance at 500 nm on a Spectronic 20 spectrophotometer. Cells were harvested after approximately 24 h of growth.

4.3. Preparation of purified DKCMO isozymes

Cells were harvested by centrifugation at 5000 g for 30 min and the cell paste from 10 L of growth medium was resuspended in phosphate buffer (pH 7.1, 21 mM; 360 ml) containing 2.5 mM β-mercaptoethanol and 100 μM EDTA. The cells were disrupted by sonication at an amplitude of 18 μ for four 30 s periods with 1 min intervals in an ice-bath. The cell debris was removed by centrifugation (21,000*g*, 20 min) and the supernatant taken to 50% ammonium sulfate saturation and left for 1 h at 4°C. The precipitate was centrifuged (21,000*g*, 20 min) and the pellet discarded. The supernatant was taken to 75% ammonium sulfate saturation and left for 1 h at 4°C. The precipitate was centrifuged as before and the supernatant discarded. The pellet was dissolved in the minumum of phosphate buffer and dialysed against two sequential 5 L aliquots of the same to remove all the salt and the native cofactor. The concentrated dialysate was then loaded to a Fast-Flow Q-Sepharose anion exchange column. Elution was effected with a gradient of 0–0.5 M KCl in phosphate buffer using a Biologic FPLC system.. Column fractions were monitored for protein concentration (A_{280}) and assayed for (+)- and (−)-camphor oxidation activity using the method of Jones et al.[28] Fractions containing protein capable of oxidising (+)-

camphor (2,5-DKCMO) were eluted in the 0.20–0.25 M KCl region of the gradient, whereas fractions capable of oxidising (−)-camphor (3,6-DKCMO) were eluted at higher salt concentrations (0.35–0.40 M). Fractions containing separated isozymes were pooled, the protein precipitated (90% saturation with ammonium sulfate), harvested by centrifugation (21,000*g*, 20 min), and then stored at 4°C until required to perform biooxidations with test substrates.

4.4. General procedure for biotransformation with purified DKCMO isozymes

A standard biotransformation mixture was used routinely: 0.9 ml of either 2,5-DKCMO or 3,6-DKCMO (<1 Unit), 0.1 ml NADH in buffer (11 μmol in pH 7.1 21mM phosphate buffer), 5 μl FMN solution (10^{-2} μmol in pH 7.1 21mM phosphate buffer), and 5 μl test sulfide (10 μmol in absolute ethanol). This mixture was placed on an orbital shaker (50 rpm) for 24 h at 25°C. A 200 μl sample was then removed to monitor substrate and product(s) concentration(s), and the remainder used to determine the enantiomeric excess and absolute configuration of the predominant sulfoxide.

4.5. Isolation and characterisation of products

To assay stopped reaction mixtures for sulfide, sulfoxide and sulfone concentrations, the 200 μl sample of a stopped reaction mixture was added an equal volume of ethyl acetate containing an appropriate internal standard, and the mixture vortexed (1 min) and then centrifuged (13,000*g*, 3 min). A 1 μl sample of the organic layer was then assayed by GLC (Shimadzu 14A GC, BP1 non-polar dimethyl siloxane column). Commercially available alkyl aryl sulfones (ethyl phenyl sulfone, methyl phenyl sulfone, or methyl tolyl sulfone) were used as internal standards. For analysis of the enantiomeric excess and absolute configuration of the predominant sulfoxide product, the remainder of a stopped reaction mixture was extracted using five volumes of ethyl acetate. The resultant organic extracts were pooled, dried using anhydrous magnesium sulfate, evaporated in vacuo, and then columned through a Pasteur pipette filled with silica gel to remove residual sulfide and polar contaminants. The eluant was concentrated (evaporation in vacuo) and then assayed either by GLC (Lipodex D or Lipodex E column), optical rotation, or ^{1}H NMR.

4.6. Source of substrates

Sulfides **7**, **8** and **19** (HLH), **22** and **23** (DV/SC), and **6** (PR) were synthesised and supplied by Prof. H. L. Holland, Dr. D. Varley/Prof. S. Colonna and Dr. P. Richardson respectively. All other sulfides were sourced at the highest quality available from commercial suppliers. The equivalent enantiomerically enriched (*S*)-sulfoxides for **1**, **2**, **17**, **18**, **19**, and **21** and (*R*)-sulfoxides for **5**, **7**, **9**, **10**, **11**, **12** and **13** were supplied by HLH and DV. Equivalent racemic sulfoxides were either synthesised using MCPBA or supplied by HLH, DV/SC or PR.

Acknowledgements

We are grateful to Profs. H. L. Holland and S. Colonna and Drs. D. Varley and P. Richardson for providing us with various sulfides and sulfoxides. Financial support was provided by the BBSRC of the UK.

References

1. Willetts, A. *Trends in Biotechnology*, **1997**, 15, 55.
2. Baeyer, A.; Villiger, V. *Ber. Dtsch. Chem.*, **1899**, 32, 3625.
3. Latham, J. A.; Walsh, C. *J. Am. Chem. Soc.*, **1987**, 109, 3421.
4. Grogan, G. Ph.D Thesis, University of Exeter, 1995.
5. Donaghue, N. A.; Norris, D. B.; Trudgill, P. W. *Eur. J. Biochem.*, **1976**, 63, 175.
6. Taschner, M. J.; Chen, Q.-Z. *Bioorg. Med. Chem.*, **1991**, 1, 535.
7. Colonna, S.; Gaggero, N.; Casella, L.; Carrea, G.; Pasta, P. *Tetrahedron: Asymmetry*, **1992**, 3, 95.
8. Alphand, V.; Furstoss, R. In *Enzyme Cataysis in Organic Synthesis*; Drauz, K.; Waldmann, H., Eds.; VCH: 1995, p. 745.
9. Chen, Y.-C.; Peoples, O. P.; Walsh, C. T. *J. Bacteriol.*, **1988**, 170, 781.
10. Jones, J. B.; Jakovac, I. J. *Can. J. Chem.*, **1982**, 60, 19.
11. Alphand, V.; Furstoss, R. *Tetrahedron: Asymmetry*, **1992**, 3, 379.
12. Carnell, A. J.; Roberts, S. M.; Sik, V.; Willetts, A. *J. Chem. Soc., Perkin Trans. 1*, **1991**, 2385.
13. Taschner, M. J.; Peddada, L.; Cyr, P.; Chen, Q.-Z.; Black, D. J. In *Microbial Reagents in Organic Synthesis*; Servi, S., Ed.; Kluwer Academic: 1992, p. 347.
14. Ottolina, G.; Pasta, P.; Carrea, G.; Colonna, S.; Dallaville, S.; Holland, H. L. *Tetrahedron: Asymmetry*, **1995**, 6, 1375.
15. Kelly, D. R. *Tetrahedron: Asymmetry*, **1996**, 7, 365.
16. (a) Ottolina, G.; Carrea, G.; Colonna, S.; Ruckemann, A. *Tetrahedron: Asymmetry*, **1996**, 7, 1123. (b) Ottolina, G.; Pasta, P.; Varley, D.; Holland, H. L. *Tetrahedron; Asymmetry*, **1996**, 7, 3427.
17. Kelly, D. R.; Knowles, C. J.; Hadhi, J. G.; Taylor, I. N.; Wright, M. A. *Tetrahedron: Asymmetry*, **1996**, 7, 365.
18. Gagnon, R.; Grogan, G.; Roberts, S. M.; Villa, R.; Willetts, A. *J. Chem. Soc., Perkin Trans. 1*, **1995**, 1505.
19. Horowitz, N. H. *Proc. Nat. Acad. Sci.*, **1945**, 31, 153.
20. Hegeman, G. D.; Rosenberg, S. L. *Ann. Rev. Microbiol.*, **1970**, 24, 429.
21. Grogan, G.; Roberts, S. M.; Wan, P.; Willetts, A. *Biotechnol. Lett.*, **1993**, 15, 913.
22. Grogan, G.; Roberts, S. M.; Willetts, A. *J. Chem. Soc., Chem. Commun.*, **1993**, 699.
23. Grogan, G.; Roberts, S. M.; Wan, P.; Willetts, A. *Biotechnol. Lett.*, **1994**, 16, 1173.
24. Gagnon, G.; Grogan, G.; Levitt, M. S.; Roberts, S. M.; Wan, P.; Willetts, A. *J. Chem. Soc., Perkin Trans. 1*, **1995**, 2537.
25. Gagnon, R.; Grogan, G.; Groussain, E.; Pedragosa-Moreau, S.; Richardson, P.; Roberts, S. M.; Wan, P.; Willetts, A.; Alphand, V.; Lebreton, J.; Furstoss, R. *J. Chem. Soc., Perkin Trans. 1*, **1995**, 2527.
26. Beecher, J.; Grogan, G.; Roberts, S.; Willetts, A. *Biotechnol. Lett.*, **1996**, 18, 571.
27. Beecher, J. Ph.D Thesis, University of Exeter, 1998.
28. Jones, K. H.; Smith, R. T.; Trudgill, P. W. *J. Gen. Microbiol.*, **1993**, 139, 797.
29. Holland, H. L. In *Organic Synthesis with Oxidative Enzymes*; VCH: 1992, p. 255.
30. Branden, C.; Tooze, J. In *Introduction to Protein Structure*; Garland Publishing: 1991, p. 141.
31. HyperChem from HYPERCUBE INC., Waterloo, Ontario, Canada. Minimisations were done in vacuo using the Polak–Ribiere algorithm, which is a cojugate gradient method: the maximum number of cycles was set for 390 and the RMS gradient default value was 0.1 kcal[A mol].
32. Holland, H. L.; Brown, F. M.; Lakshmaiah, G.; Larsen, B. G.; Patel, M. *Tetrahedron: Asymmetry*, **1997**, 8, 683.
33. Freutel, J.; Chang, Y.-T.; Collins, J.; Loew, G.; Ortiz de Montellano, P. R. *J. Am. Chem. Soc.*, **1994**, 116, 11643.
34. Harris, D.; Loew, G. *J. Am. Chem. Soc.*, **1995**, 117, 2738.
35. Poulos, T. L.; Finzel, B. C.; Gunsalus, I. C.; Wagner, G. C.; Kraut, J. *J. Biol. Chem.*, **1985**, 260, 16122.
36. Walsh, C. T.; Chen, Y.-C. J. *Angew. Chem. Int. Ed. Engl.*, **1988**, 27, 333.
37. Deslongchamps, P. In *Stereoelectronic Effects in Organic Chemistry*; Pergamon: Oxford, 1983, p. 124.
38. Conrad, H. E.; Dubus, R.; Namdtvedt, M. J.; Gunsalus, I. C. *J. Biol. Chem.*, **1965**, 240, 495.